Proceedings of the 29th Polish-Slovak Scientific Conference on Machine Modelling and Simulations 2024, Poland

Analytical–Numerical Methods of Predicting the Mechanical Properties of Welded Joints Made of Steel

Z. Saternus[a,*], W. Piekarska[b], M. Kubiak[a] and T. Domański[a]

[a] *Czestochowa University of Technology, Faculty of Mechanical Engineering, Dąbrowskiego 69, 42-201 Częstochowa, Poland*
[b] *Academy of Silesia, Faculty of Architecture, Civil Engineering and Applied Arts, Rolna 43, 40-555 Katowice, Poland*

Doi: 10.12693/APhysPolA.145.751 *e-mail: zbigniew.saternus@pcz.pl

The work concerns an analysis of phase transformations in the solid state and the prediction of the structure and mechanical properties of steel using analytical models and numerical methods. The analytical models involve building simplified continuous cooling transformation diagrams for welding, predicting the microstructure based on the chemical composition of steel, as well as assessing the mechanical properties of the welded joint made of S1100QL steel. The kinetics of phase transformations and prediction of mechanical properties distribution in the cross-section of the joint are carried out based on analytical methods. The analytical models presented in this work replace the classic mathematical models of phase transformation kinetics and interpolated experimental continuous cooling transformation diagrams (time–temperature transformation). The analytical relationships presented in the work are determined by the chemical composition of the steel and the cooling time $t_{8/5}$. Based on the chemical composition of the steel, the continuous cooling transformation diagrams and the specific volume fractions of phases as a function of the cooling time $t_{8/5}$ of the steel are determined. The numerical simulation of the welding process of sheets made of S1100QL steel is carried out in Abaqus software using DFLUX and HEATVAL numerical subroutines. The calculations use the mathematical model of Goldak's volumetric welding source power distribution. Thermal cycles and temperature field are numerically determined. The research results obtained in this work are compared with the experimental results.

topics: continuous cooling transformation (CCT) diagram, phase transformation, numerical analysis, analytical model

1. Introduction

The analysis of phase transformations of steel and the determination of the resulting deformations during the welding process are usually performed based on classical mathematical models of the phase transformation kinetics and interpolated experimental CCT (continuous cooling transformation) diagrams [1–6].

The cooling curves from the diagrams are written in the form of mathematical equations. This approach requires performing many dilatometric tests and preparing experimental diagrams for a given steel, which is very time-consuming and very expensive. Such studies can be replaced by results obtained using analytical methods. The analytical relationships are determined by the chemical composition of the steel and the cooling time $t_{8/5}$. Based on the chemical composition of the steel, the CCT diagram can be determined, and the volume fractions of the phases can be determined as a function of the cooling time $t_{8/5}$ of the steel [7–11].

The analytical models presented in this paper concern the development of simplified CCT diagrams, prediction of the structure based on the chemical composition of steels from the group of weldable steels, and assessment of the mechanical properties of the welded joint. The developed calculations were based on the example of S1100QL steel.

2. Analytical models of phase transformations

The empirical formulas presented in the paper were determined by means of statistical analysis of the set of results of a series of experimental tests for specific material groups [10, 11]. Empirical formulas can be used to determine characteristic values of austenite transformation during cooling in the welding process. Values such as the beginning temperatures of phase transformations during heating and cooling and the times of the start and finish of the occurrence of individual phases can be determined.

The analytical relationships in the work concern steel S1100QL, with chemical composition: 0.18 C, 0.50 Si, 16 Mn, 1.45 Cr, 2.39 Ni, 0.12 V, 0.017 P, 0.003 S. In all empirical formulas, the symbols of chemical elements indicate the percentage of a given element in the steel, e.g., C $\Rightarrow$ %C.

To construct analytical CCT diagrams, the beginning temperatures of individual transformations and the start times of these transformations are needed. These values are determined based on the chemical composition of the steel. The maximum temperature of the thermal cycle was assumed as the austenitization temperature ($T_{\text{aust}} = T_{\max}$) [11, 12]. For the group of steels that includes S1100QL steel, the temperatures of the beginning of the formation of ferrite $F_s(t)$, bainite $B_s(t)$, pearlite $P_s(t)$, and the finish temperature of the transformation $T_k(t)$, dependent on time ($t = t_{8/5}$), according to the authors of [7, 8, 10, 11] are obtained from the equations

$$B_s(t) = T_{B0} + \Delta T_B \operatorname{erf}\Big[\big(\ln(t) - \ln(t_{B0})\big)K_B\Big] + K_{Bt}\ln(t) \;\Rightarrow\; T_{B0} = T_{B0}(t) = M_s, \quad (1)$$

$$F_s(t) = T_{F0} + \Delta T_F \operatorname{erf}\Big[\big(\ln(t) - \ln(t_{F0})\big)K_F\Big] + K_{Ft}\ln(t) \;\Rightarrow\; T_{k0} = T_{k0}(t) = M_s, \quad (2)$$

$$P_s(t) = T_{P0} + \Delta T_P \operatorname{erf}\Big[\big(\ln(t) - \ln(t_{P0})\big)K_P\Big] + K_{Pt}\ln(t) \;\Rightarrow\; T_{F0} = B_s(t_{F0}), \quad (3)$$

$$T_k(t) = T_{k0} + \Delta T_k \operatorname{erf}\Big[(\ln(t) - \ln t_{k0})K_k\Big] + K_{kt}\ln(t) \;\Rightarrow\; T_{P0} = B_s(t_{P0}). \quad (4)$$

The values of ΔT_B, K_B, ΔT_F, K_F, ΔT_P, K_P, ΔT_k, and K_k depend on the chemical composition of the tested steel.

The temperatures of the beginning and finish of the martensitic transformation (respectively, M_s and M_f) can be determined as follows [10, 11]

$$M_s = 530 - 415\text{C} + 90\text{C}^2 - 35\text{Mn} - 30\text{Cr} - 20\text{Ni} - 15 - 15\text{W} - 10\text{Mo}, \quad (5)$$

$$M_f = 381.76 - 252.44\text{C} - 111.12\text{Mn} + 54.538\text{Si} + 114.17\text{Cr} - 23.779\text{Ni} - 57.381\text{Mo} + 215.7\text{V} + 945.4\text{Nb} + 1821.7\text{Ti} - 1746.5\text{B}. \quad (6)$$

The initiation times of individual phase transformations: ferrite t_F, pearlite t_P, and bainite t_B, are determined from the relationship

$$t_B = -1.8 + 28.3\text{C} + 17.1\text{Mn} - 59.6\text{Si} - 20\text{Cr} + 13.2\text{Ni} + 0.1\text{Mo} - 5.3\text{V} + 47.0\text{Nb} - 289.6\text{C}^2 - 3.7\text{Mn}^2 + 65.4\text{Si}^2 + 38.6\text{Cr}^2 - 7.0\text{Ni}^2 - 21.0\text{Mo}^2 + -9.8\text{CMn} - 19.5\text{MnSi} + 232.1\text{CSi}, \quad (7)$$

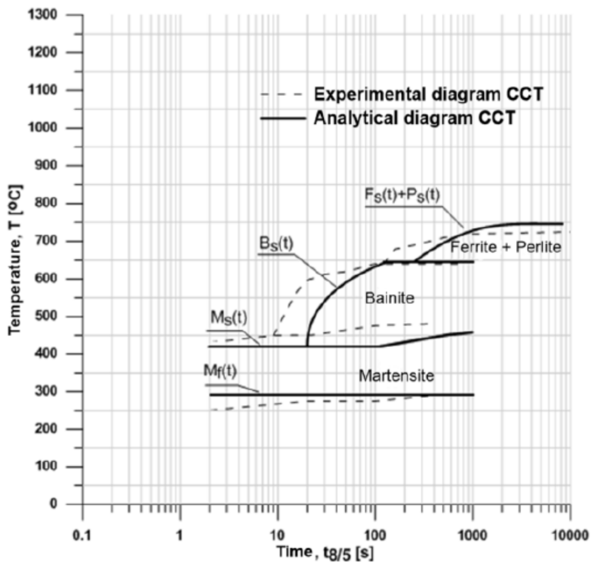

Fig. 1. CCT diagram of S1100QL steel.

$$t_F = 10^{\left[5.8\left(\text{C}+\frac{\text{Si}}{291}+\frac{\text{Mn}}{14}+\frac{\text{Ni}}{67}+\frac{\text{Cr}}{16}+\frac{\text{Mo}}{6}+\frac{\text{V}}{425}\right)-0.83\right]}, \quad (8)$$

$$t_P = 10^{\left[5.14\left(\text{C}+\frac{\text{Si}}{17}+\frac{\text{Mn}}{19}+\frac{\text{Ni}}{25}+\frac{\text{Cr}}{16}+\frac{\text{Mo}}{4}+\frac{\text{V}}{3}\right)+0.06\right]}. \quad (9)$$

The analytical and experimental CCT welding diagrams are shown in Fig. 1.

The CCT diagram is the basis for the analysis of phase transformations in the welding process, i.e., predicting the structural composition of the entire joint and its properties. The cooling times and determined volume fractions of the individual phases as a function of the cooling time $t_{8/5}$ are the input data for numerical calculations of deformations and stresses generated during the welding process.

3. Analytical methods for determining the mechanical properties of welded joints

The mechanical properties can be determined based on the structural composition and properties of each structure. If the phase composition of the material is known, and more precisely, the share of individual phases (ferrite–pearlite, martensite, and bainite) and the properties of individual structural components W_i, the properties of the entire zone can be predicted with high probability [9–11]. The component W may represent hardness, yield strength, tensile strength, constriction or elongation,

$$W = \sum\nolimits_{i=M,B,F,P} W_i\,\eta_i. \quad (10)$$

The mechanical properties of individual structural components are determined by the chemical composition of the tested steel. The yield strength (Re_i), tensile strength (Rm_i), elongation (A_i) and reduction of area (Z_i) can be determined using the following empirical formulas [9–11]

$$Re_{FP} = 187 + 92\text{C} + 47\text{Mn} + 90\text{V},$$
$$Re_{M} = 602 + 2150\text{C} + 500\text{Mo},$$
$$Re_{B} = 500 + 460\text{C} - 120\text{C}^2 + 150\text{V} + 360\text{Mo}, \quad (11)$$

$$Rm_{FP} = 297 + 1360\text{C} + 60\text{Mn} + 140\text{V},$$
$$Rm_{M} = 798 + 3215\text{C},$$
$$Rm_{B} = 590 + 960\text{C} + 39.7\text{Mn} + 200\text{V}, \quad (12)$$

$$A_{M} = 12.267\text{C}^2 - 1.5\text{Mn} + 0.76\ln(t),$$
$$A_{B} = 21.3 - 35.6\text{C} - 4.0\text{Mn} - 5.0\text{V} + 1.84\ln(t),$$
$$A_{FP} = 36.5 - 127\text{C} + 153\text{C}^2 - 1.16\text{Mn} + 8.0\text{V} + 0.66\ln(t), \quad (13)$$

$$Z_{FP} = 65.4 - 88\text{C} - 82\text{C}^2 - 6.7\text{Mn} + 18\text{V} + 0.6\ln(t),$$
$$Z_{M} = 48.5 - 158\text{C} + 116\text{C}^2 - 0.98\ln(t),$$
$$Z_{B} = 53.3 - 132\text{C} + 103\text{C}^2 - 5.1\text{Mn} - 10\text{V} + 3.4\ln(t). \quad (14)$$

Hardness is one of the basic values that characterizes a given welded joint. The hardness (HV_i) of individual structural components can be determined using the formulas given by the authors of works [10, 11] as a function of the chemical composition of the steel and the speed $v_{8/5}$ (where $v_{8/5} = (800 - 500)/t_{8/5}$)

$$HV_{FP} = 42 + 223\text{C} + 53\text{Si} + 30\text{Mn} + 12.6\text{Ni} + 7\text{Cr} + 19\text{Mo} + (10{-}19\text{Si}{+}4\text{Ni}{+}8\text{Cr}{+}130\text{V})\log(\nu_{8/5}),$$

$$HV_{M} = 127 + 959\text{C} + 27\text{Si} + 11\text{Mn} + 8\text{Ni} + 16\text{Cr} + 21\log(\nu_{8/5}),$$

$$HV_{B} = -323 + 185\text{C} + 330\text{Si} + 153\text{Mn} + 65\text{Ni} + 144\text{C} + 191\text{Mo} + \big(89 + 53\text{C} - 55\text{Si} - 22\text{Mn} - 10\text{Ni} - 20\text{Cr} - 33\text{Mo}\big)\log(\nu_{8/5}). \quad (15)$$

The authors of [13–15] conducted experimental studies of S1100QL steel. The structure and mechanical properties were determined. The structure of the analyzed steel (Fig. 2, see also [13]) consists of fine-grained martensite (grain diameter of about 1–8 mm), bainite, and a trace amount of ferrite; assumed: 20%M, 75%B, and 5% ferrite.

Using the relations (10)–(15) and information on the structure of the base material, the mechanical properties of the base material were analytically determined. The analytical calculation results and experimental results are presented in Table I.

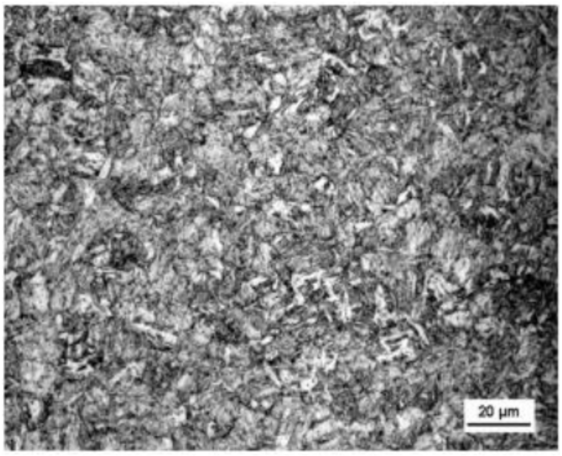

Fig. 2. Microscopic image of the base material of S1100QL steel [13].

TABLE I

Mechanical properties of S1100QL steel.

Research results	HV	Re [MPa]	Rm [MPa]	A [%]	Z [%]
Experimental research [13]	320	1120	1430	12.5	58
Analytical methods	318	1139	1377	15.05	48.02

4. Temperature field, phase transformations

This paper presents an example of predicting the hardness distribution in the cross-section of a flat bar made of S1100QL steel butt-welded with an electric arc. The temperature field of the welded joint was determined using the Abaqus FEA engineering software based on the finite element method (FEA). Thermal analysis in the computational program is based on the law of energy conservation and Fourier's law [16].

The modeling of the moving welding source was implemented in the Abaqus FEA software. The temperature field and thermal cycles in the welded joint were numerically determined using the DFLUX and the HEATVAL numerical subroutines [1, 6, 16]. The standard form of the Abaqus FEA program requires the implementation of additional proprietary numerical procedures. In the DFLUX numerical subroutine, the power distribution of the moving welding source is modeled using mathematical equations. In the HEATVAL subroutine, the thermal cycle parameters are determined, i.e., heating and cooling times and the maximum cycle temperature. The numerical analysis of phase transformations in the solid state and the prediction of the structural composition in the welding process are performed in the additional UEXPAN procedure. For the temperature field calculations, the source power $Q = 2200$ W and welding speed $v = 10$ mm/s were assumed. A mathematical model of a volumetric welding source with the Goldak distribution was used in the calculations [2, 17]. Numerical calculations of the temperature field were performed

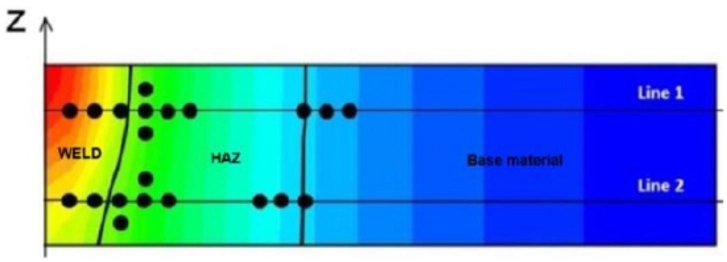

Fig. 3. Cross-sectional area with measurement points.

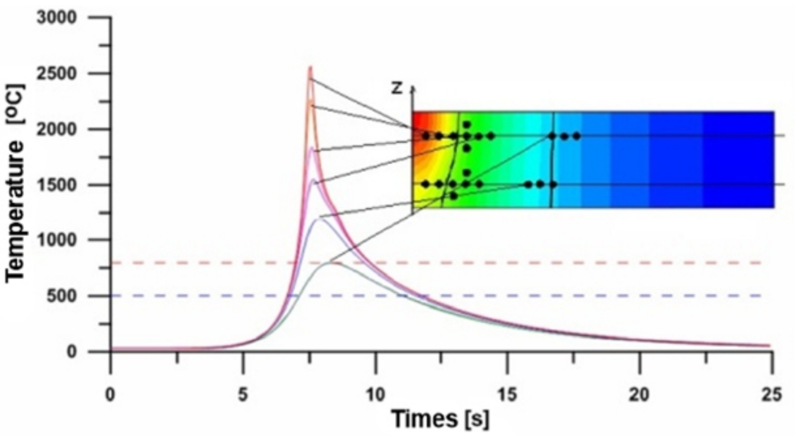

Fig. 4. Welding thermal cycles for selected measurement points.

as a three-dimensional problem. On the basis of the numerically determined temperature distribution, the mechanical properties in the welded joint were predicted.

5. Results of the research

The analysis of the hardness distribution and other mechanical properties was carried out for selected points of the welded joint cross-section (Fig. 3) in two different measuring lines (marked in the figure as Line 1 and Line 2). For these points, cooling times $t_{8/5}$ were also determined using calculated thermal cycles (Fig. 4). The prediction of mechanical properties in the weld and in the heat-affected zone (HAZ) of the welded joint was carried out based on equations (10)–(15) and the analytically obtained volume fractions of the individual phases as a function of the cooling time $t_{8/5}$.

The hardness distribution in the welded joint, both determined analytically and as a result of experimental tests presented by the authors of [15], is illustrated in Fig. 5.

Analytically predicted mechanical properties in the cross-section of the joint (yield strength (Re), tensile strength (Rm), elongation (A) and reduction of area (Z)) in the weld and in the HAZ of the welded joint (measurement Line 1, marked in Fig. 3) are shown in Fig. 6.

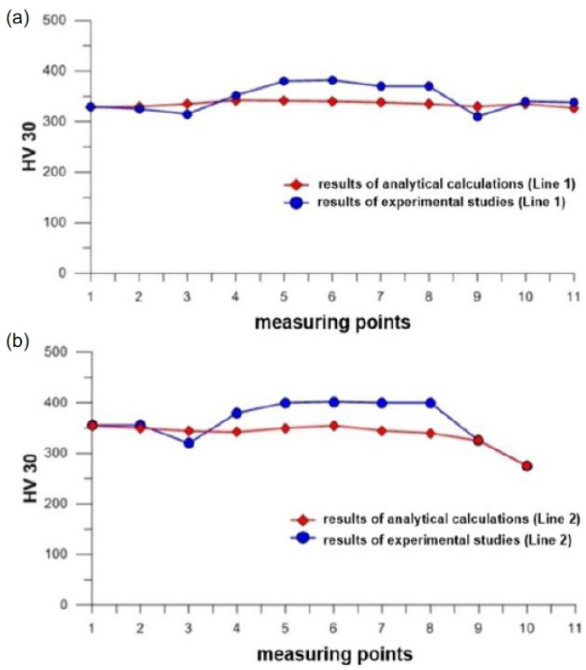

Fig. 5. Comparison of hardness distributions obtained analytically with experimental studies, (a) measurement Line 1, (b) measurement Line 2.

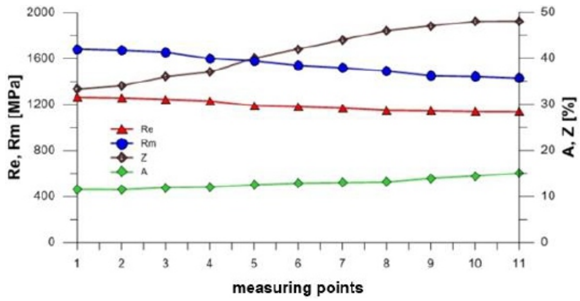

Fig. 6. Numerically estimated distribution of mechanical properties in the cross-section of the joint.

6. Conclusions

This paper evaluates the usefulness of using analytical methods to predict the structure and mechanical properties of a welded joint. An analytical CCT diagram of S1100QL steel was constructed and verified experimentally. A numerical example is presented using quantities determined by analytical methods.

Based on the numerical simulation, the temperature field was determined. Individual zones of the joint and mechanical properties of the electric arc welded joint of S1100QL steel were determined. Based on the determined volume fractions and analytical models determining the mechanical properties of individual structures, the distributions of *Re*, *Rm*, *A*, *Z*, and *HV* in the cross-section of the welded joint were numerically predicted.

Comparison of analytical results with experimental results shows that analytical methods can be used for preliminary analysis of material properties intended for welded structures. They can also be used as input data in numerical methods for determining stresses and deformations of welded elements, replacing expensive and laborious experimental studies.

References

[1] N. S. Bailey, Ch. Katinas, Y. C. Shin, *J. Mater. Process. Tech.* **247**, 223 (2017).

[2] F. Zhao, J. Huang, Z. Zhang, *Optics & Laser Technology* **181**, 112010 (2025).

[3] J. Brabec, Š. Ježek, L. Beneš, A. Kříž, P. Majrich, *Manufacturing Technology* **21**(1), 29 (2021).

[4] V.I. Makhnenko, E.A. Velikoivanenko, O.V. Makhnenko, G.F. Rozynka, N.I. Pivtorak, Issledovanie vlijanija fazovych prevrascenij na ostatocnye naprjazenija pri svarke kol'cevych stykov trub. *Avtomat. Svarka* **5**, 3-8 (2000).

[5] H. Sun, Y. Han, Z. Sun, Z. Dong, R Lang, *J. Manuf. Process.* **120**, 1192 (2024).

[6] W. Piekarska, M. Kubiak, Z. Saternus, *Arch. Metall. Mater.* **57(4)**, 1219 (2012).

[7] P. Seyffart, O.G. Kasatkin, *Mathematisch-statistische Beschreibung der Austenitumwandlung in der Wärmeeinflußzone, Schweißtechnik* **29**, 117 (1979).

[8] P. Seyffart, O.G. Kasatkin, *Avtomat. Svarka* **1**, 7 (1984).

[9] P. Seyffart, O.G. Kasatkin, *Rascentnye modeli dla ocenki mechaniceskich svojstv metalla ZTV pri svarke nizkoegirovannych stalej, Proc. Int. Conference mechanical Modelling and Information Technologies in Welding and Related Processes*, ed. V.I.Makhnenko, Katsiveli, Crimea, E.O. Paton Welding Inst. of NAS of Ukraine, pp. 103-106, Kiev 2002.

[10] J. Mikuła, *Analityczne metody oceny spawalności stali, zeszyty naukowe Mechanika nr 85*, Politechnika Krakowska, Kraków, 2001.

[11] W. Piekarska, *Analiza numeryczna zjawisk termomechanicznych procesu spawania laserowego. Pole temperatury, przemiany fazowe i naprężenia, seria Monografie* nr 135, Wydawnictwo Politechniki Częstochowskiej, Częstochowa, 2007 (in Polish).

[12] W. Piekarska, D. Goszczyńska, Z. Saternus, *J. Appl. Math. Comput. Mech.* **14(2)**, 61 (2015).

[13] J. Nowacki, A. Sajek, P. Matkowski, *Arch. Civ. Mech. Eng.* **16**, 777 (2016).

[14] T. Ślęzak, L. Sniezek, *Key Engineering Materials* **598**, 237 (2024).

[15] I. Samardžić, A. Ćorić, M. Dunđer, *Metalurgija* **55**, 453 (2016).

[16] SIMULIA Dassault System, Abaqus theory manual, Version 6.7, 2007.

[17] J.A. Goldak, *Computational Welding Mechanics*, Springer NY, 2005.